Supporting Material

Atomic Scale Variations of the Mechanical Response on 2D Materials Sensed by Non-Contact AFM.

B. de la Torre‡[1], M. Ellner‡[2], P. Pou[2,3], N. Nicoara[1,4], Rubén Pérez*[2,3] and J. M. Gómez-Rodríguez*[1,3,5]

[1]Departamento de Física de la Materia Condensada, Universidad Autónoma de Madrid, Spain

[2]Departamento de Física Teórica de la Materia Condensada, Universidad Autónoma de Madrid, Spain

[3]Condensed Matter Physics Center (IFIMAC), Universidad Autónoma de Madrid, Spain

[4]Iberian Nanotechnology Laboratory, Braga, Portugal

[5]Instituto Nicolás Cabrera, Universidad Autónoma de Madrid, Spain

1. Experimental methods.

The experiments were performed with a home-made ultra-high vacuum cantilever based NC-AFM operated at 5 K. In this setup, optical interferometry is used to detect the dynamics of the cantilever. The AFM was operated using the frequency modulation method, where the shift of the cantilever free resonance frequency is measured, while keeping constant the oscillation amplitude. Large oscillation amplitudes (10-20 nm) were required to maintain the stability of the cantilever during the measurements. A sample voltage (V_{bias}) was established to minimize the long-range electrostatic force at the beginning of the acquisition. The microscope was controlled by DULCINEA SPM controller (Nanotec electronica S.L.) in combination with the easy PLL plus controller (Nanosurf). Simultaneous images and 2D mapping were performed using the WSxM software [1]. Simultaneous images, using the second pass method, were performed by acquiring the fast scan direction in topography images twice at two different set point before moving the tip in the slow scan direction. The 2D mapping was recorded along 128 points on the graphene surface. During the acquisition, the tip is required to move parallel to the surface without topographic feedback. After a forward movement, the tip is displaced in Z direction an amount of 1 nm/128 points = 7.8 pm up to a distance of 1 nm. Each 2D mapping takes about 4 minutes so thermal drift has no impact in our data (typical drift ~0.03 nm/h). All the data was analyzed using the WSxM software [1].

Epitaxial graphene on platinum (111) was grown from ethylene chemical vapor deposition (CVD) in ultra-high vacuum. The Pt(111) surface was cleaned by several cycles of argon ion sputtering at 1 keV and annealing at 900 K followed by a flash heating up to 1300 K in oxygen pressure (2×10^{-7} Torr). After obtaining a clean Pt(111) surface, graphene was grown in situ by ethylene decomposition ($P = 3\times10^{-7}$ Torr; 60 s) while keeping the surface at ~1300 K. With this procedure, we were able to grow very large graphene regions on Pt(111) [2].

Commercial platinum-iridium covered silicon cantilevers (NCLPt Nanosensors; resonance frequency ~160 KHz, k ~ 30 N/m) were cleaned of impurities in ultra-high vacuum by Ar^+ ion sputtering (0.6 keV). The spring constant k is calculated from the geometrical dimensions of the cantilever and its eigenfrequency [3].

It has been argued [4] that instrumental artifacts could sometimes lead to spurious effects in dissipation measurements. In order to assess the validity of our present measurements, we have checked the reproducibility of the dissipation signal using several different cantilevers and tips (being all PtIr covered Silicon Cantilevers PPP-NCLPt from Nanosensors). With all of them, we found the same step-like increase of the dissipation signal as the one shown in fig. 2 of the main manuscript, with a plateau at shorter distances. The average value of the dissipation at this plateau obtained using 6 different cantilevers and tips is 0.86 +/- 0.09 eV/cycle, which is completely consistent with the particular value (corresponding to a given cantilever and tip) shown in the main manuscript. These measurements were obtained at different frequency shifts and oscillation amplitudes (ranging from 10 to 20 nm). Moreover, this dissipation signal was not present on dissipation measurements performed on other surfaces, different from G/Pt(111), measured under similar frequency ranges. All these facts justify our assumption of a negligible influence of possible transfer function spurious effects in the present data.

2. DFT calculations details

The investigation of the 3×3 Graphene/Pt(111) moiré was performed with the DFT code OpenMX [5], that is formulated on a localized orbital basis. Standard GGA-PBE XC functional with DFT-D3 [6] vdW energy and gradients corrections (implemented into the code by our group) was used. A double-zeta polarized (DZP) basis set was used for all atoms. A 7 au cut-off radius was used for both the C atoms and the Pt on the substrate and 9 au for the Pt on the tip. The k-sampling of the Brillouin zone was discretized with 3×3×1 grids. A dense real space grid E_{grid} = 200×200×300 Ry and a stringent electronic convergence criterium ($E^{SCF} = 10^{-6}$ Ha) were used. The calculations included geometry relaxation of all the atoms of the system apart from the top layer of the tip and the bottom layer of the Pt slab. Atomic relaxations were stopped when forces on individual atoms were smaller than $F_{max} = 2 \times 10^{-4}$ Ha a_0^{-1}. With this choice of basis set and accuracy parameters, the G's lattice constant (LC) that minimizes the energy is 2.475Å. All calculations retain G's DFT LC, and, in order to commensurate G and Pt's lattices, a 0.7% strain was applied to the Pt substrate. In order to avoid interaction between image tips, a large supercell of 6×6 Graphene/Pt with 4 layers of Pt atoms for a total of 194 atoms was used. This corresponds to a (14.85 Å, 14.85 Å, 30 Å) supercell. As for the AFM tip, in the main calculations a Pt 10 atoms apex was used.

3. Tip sample interaction in the repulsive regime

As mentioned in the main text, ionic relaxations obtained through DFT show that in the repulsive interaction regime the tip apex-G separation varies little. While the tip-sample distance is reduced, the G layer is locally deformed acting itself as a tip that allows sensing of the Pt surface. Thus, in this regime, the moiré modulation in the G layer is a result of the atomic-scale Pt-G interaction. This can be clearly observed in figure S1 where the relaxed structure of a Pt10 tip indenting onto a 6 × 6 G on 4 layers of Pt(111) is shown. Figure S1a shows the tip on a top-high site of the moiré pattern while figure S1b shows the tip is on a top-low site. As mentioned in the main text, the high/low area of the moiré is determined by the G environment with respect to the Pt substrate: the high area corresponds to a C atom whose closest environment has a hollow site of Pt(111) directly below, while the low area corresponds to a C atom with a Pt atom directly underneath. We also include in the supplementary information two movies showing the complete indentation process (from a tip-sample distance of 5.5 Å to 1 Å) for both cases.

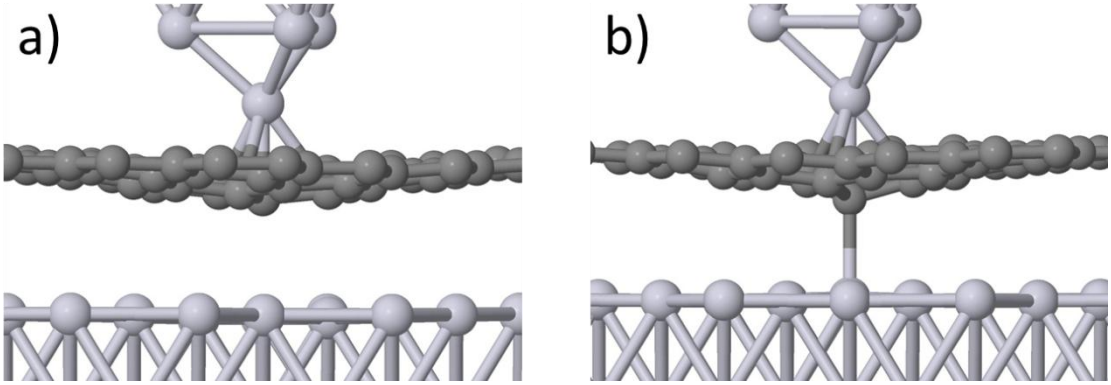

Figure S1. Relaxed atomic positions with the tip located at 1 Å above the G sheet. The tip is directly positioned on a) a top-high site and b) a top-low site of the 6 × 6 G/Pt moiré.

4. Multiscale Model for Non-Local Atomic Scale Deformations: Fittings

The multiscale model presented in the main text and described by,

$$V(z_{global}, z_{local}, z_t) = V_{t-G}(z_t - z_{local}) + A_1 V_{T-G}(z_T - z_{global}) + A_1 V_{Pt-G}^{global}(z_{global} - z_{Pt}) + V_{Pt-G}^{local}(z_{local}) + V_{BR}(z_{local} - z_{global}) + A_2 V_{E2D}(z_{global}),$$

contains the following 6 terms: the nanoscopic tip-G interaction V_{t-G}, the macroscopic tip-G interaction V_{T-G}, the interaction of global and local G areas with the Pt substrate, V_{Pt-G}^{global} and V_{Pt-G}^{local} respectively, and the interaction due to the mechanical deformations of the G sheet, V_{BR} and V_{E2D}. These interaction terms depend on three independent variables: the z-coordinate of the local deformation of the G sheet z_{local}, the z-coordinate of the global deformation of the G sheet z_{global}, and the position of the nanoscopic tip apex z_t. We have fixed the origin at the equilibrium position of the G layer on Pt without the tip. Note that z_{Pt} and z_T are fixed by the constraints $z_{Pt} = -3.35$ Å and $z_T - z_t = 3.5$ Å. A schematic representation of the interactions included in the multiscale model is shown in figure S2. Finally, we take into account the spatial area of the deformations through A_1 and A_2 parameters. These were chosen to reproduce the dissipation energy plateau from the experiments: $A_1 = 0.68$, $A_2 = 0.09$. These parameters as well as the energies calculated with DFT used for the fittings are referred to the 6×6 G cell. The parameterization of the interaction terms are described below.

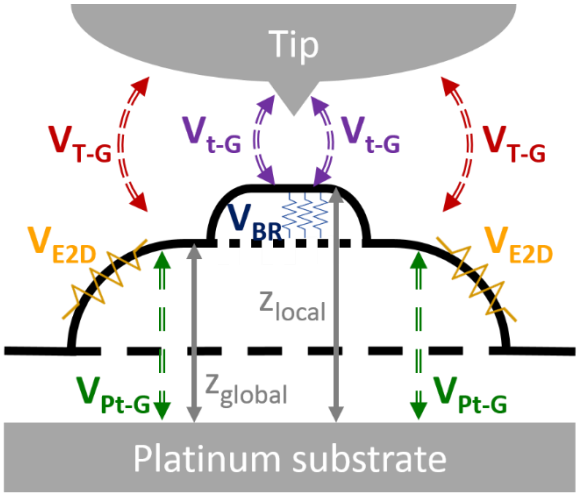

Figure S2. A scheme of the theoretical model which includes: a macroscopic and nanoscopic Pt tip, the graphene surface divided into a local and global area, and the Pt substrate. The potential depends on the position of the tip and the global and local deformations of the graphene.

1) Nanoscopic tip-G interaction V_{t-G}

This term describes the nanoscopic Pt tip-G flake interaction. It was fitted from simulations of a Pt10 (10 atom pyramid Pt tip cluster from the (111) direction) on a 6×6 G flake with all atomic positions fixed. Figure S3a shows the energy as a function of the distance between the G and the tip apex for two G sites: a top site and a hollow site. The fitting was done using a Morse potential and an integrated (over one plane) vdW term,

$$V_{t-G} = V_0((1 - exp[-k(r - r_c)])^2 - 1) - \frac{C}{r^4},$$

with $V_0 = 0.25$ meV, $k = 2.31$ Å^{-1}, $r_c = 3.82$ Å, $C = 7.37$ eVÅ^4 for the top site and $V_0 = 6.82$ meV, $k = 1.57$ Å^{-1}, $r_c = 3.59$ Å, $C = 7.26$ eVÅ^4 for the hollow site.

2) Macroscopic tip-G interaction V_{T-G}

This term describes the interaction between the macroscopic tip and the G sheet. The typical radius of the Pt coated Si tips used in the experiments is 200 nm. For the interaction of this macroscopic part with the G layer we can approximate $R_{tip} \to \infty$, for all practical purposes. Thus, we simulate the macroscopic tip-G interaction as the one originated between a 6×6 G sheet and a 4 layer Pt(111) slab. Although the main contribution is due to vdW interaction, at short tip-sample distances, a repulsive term in needed in order to describe Pauli interaction. Figure S3b shows the plot of the energy as a function of the tip-G positions along with the fitting. We fit the data using an integrated (over both planes) vdW term and a Morse potential,

$$V_{T-G} = V_0((1 - exp[-k(r - r_c)])^2 - 1) - \frac{C}{r^2},$$

with $V_0 = 1.44\ eV$, $k = 1.06$ Å^{-1}, $r_c = 3.39$ Å, $C = 3.83\ eV$Å^2.

3) Global Pt substrate-G interaction V_{Pt-G}^{global}

This term describes the interaction between the Pt substrate and the global G area. The same DFT simulation and fitting as in V_{T-G} is used.

4) Local Pt substrate-G interaction V_{Pt-G}^{local}

In order to examine the difference in force between different sites of the moiré using the multiscale model, we need an extra term to the G-substrate interaction which takes into account the mechanical energy difference due to out-of-plane deformations of the G layer from two different areas of the moiré: a high-top site and a low-top site. We calculate the difference in energy through DFT by displacing a single atom of a 6×6 G flake on 4 layer Pt(111) substrate and allowing all G atoms to relax. The difference in energy shows a linear response with respect to the displacement. However, due to the limited size of the G layer used in the simulation, after ~ 2 Å of displacement, the whole sheet starts to separate from the substrate. In order to erase this artifact form the fitting, we saturate the response at this height. Figure S3c shows the elastic energy difference due to out-of-plane deformations between the two sites of the moiré. The plot also shows the fitting which was done using

$$V_{G-Pt}^{local} = E^{low} - E^{high} = E_0 \left(\frac{1}{e^{-z-z_0} + 1} - \frac{1}{2} \right),$$

with $E_0 = 0.24\ eV$ and $E_0 = 3.35$ Å. Since we have chosen to reference this interaction with respect to the high part of the moiré, the term is only included on the low part of the moiré.

5) Elastic response of G to out-of-plane deformations $V_{BR} + V_{E2D}$

These terms describe the mechanical response of the G sheet to out-of-plane elastic deformations. Since pristine graphene is a 2D membrane, the energy versus deflection has a

quadratic relationship due to the pretension or bending rigidity V_{BR} and a quartic relationship due to the two-dimensional Young's Modulus V_{E2D} [7]. These two terms were fitted from a simulation of a 6 × 6 G sheet in which a single C atom of the G was displaced vertically and all atoms of the layer except the corner atoms were allowed to relax. Figure S3d shows the plot of the energy as a function of the displaced atom position along with the fitting. The fitting contains

$$V_{BR} + V_{E2D} = \frac{G_0}{2}\delta^2 + \kappa\delta^4,$$

with $G_0 = 1.13\ eV\text{Å}^{-2}$ and $\kappa = 0.053\ eV\text{Å}^{-4}$.

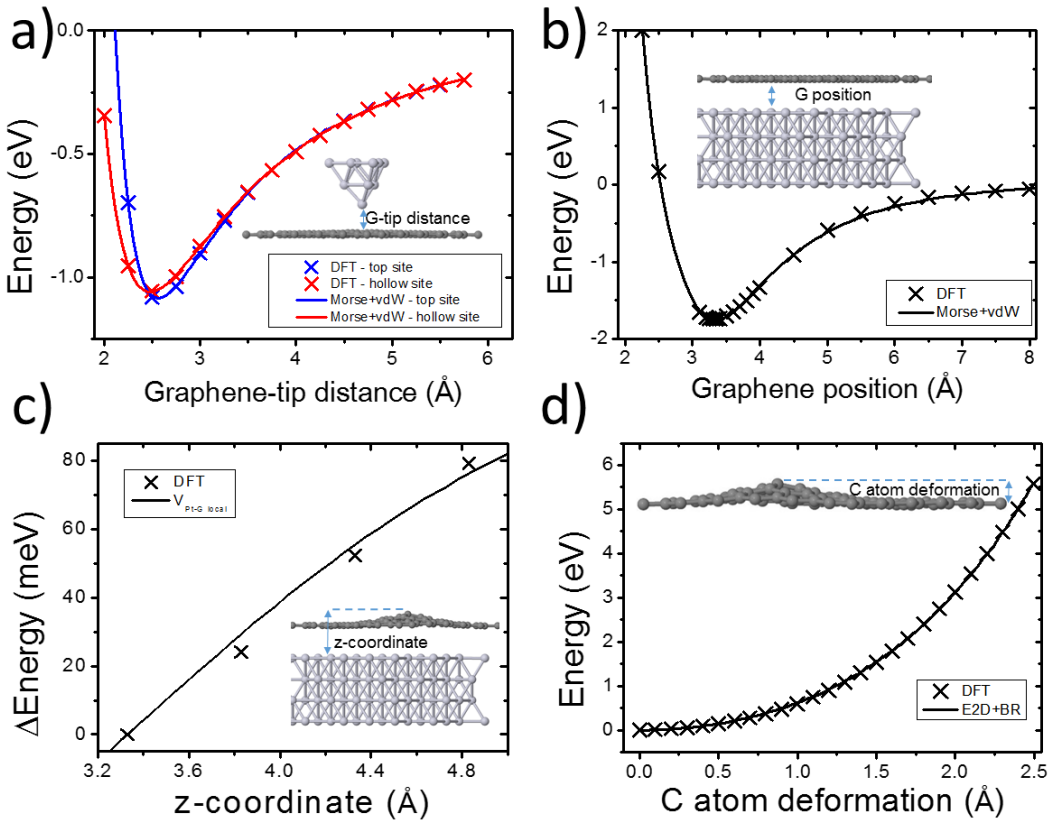

Figure S3. Fittings for the model. a) The nanoscopic-G interaction V_{t-G}, b) the macroscopic tip-G V_{T-G} and Pt substrate-G V_{Pt-G}^{global} interaction, c) the Pt-G interaction difference (V_{Pt-G}^{local}) between the high-top and low-top sites and d) the elastic response of the G to out-of-plane deformations $V_{BR} + V_{E2D}$. Crosses are the DFT results and lines the fitted contributions of the multiscale model.

5. Multiscale Model for Non-Local Atomic Scale Deformations: Dominant contributions

In order to clarify the dominant contributions that stabilize the energy minima, we plot in figure S4 the contributions to the energy along the reaction coordinate for tip-G separations (z_t) 6.5 Å, b) 5.0 Å, and c) 2.5 Å. The reaction coordinate is calculated by minimizing the total potential along z_{local}: $RC = [z_{local}^2 + z_{global}^2(V_{min})]^{1/2}$. At large z_t (figure S4a) the system presents one minimum. It comes from the G-Pt interaction, which is responsible for

binding the G to the substrate. The elastic response of the G to out-of-plane deformations oppose the nanoscopic and macroscopic tip-sample interactions that would otherwise create a second minimum, binding the G to the tip. For intermediate z_t the elastic energy decreases allowing the second minimum, primarily coming from the nanoscopic tip-G interaction, to appear. For small z_t, both minima converge into one.

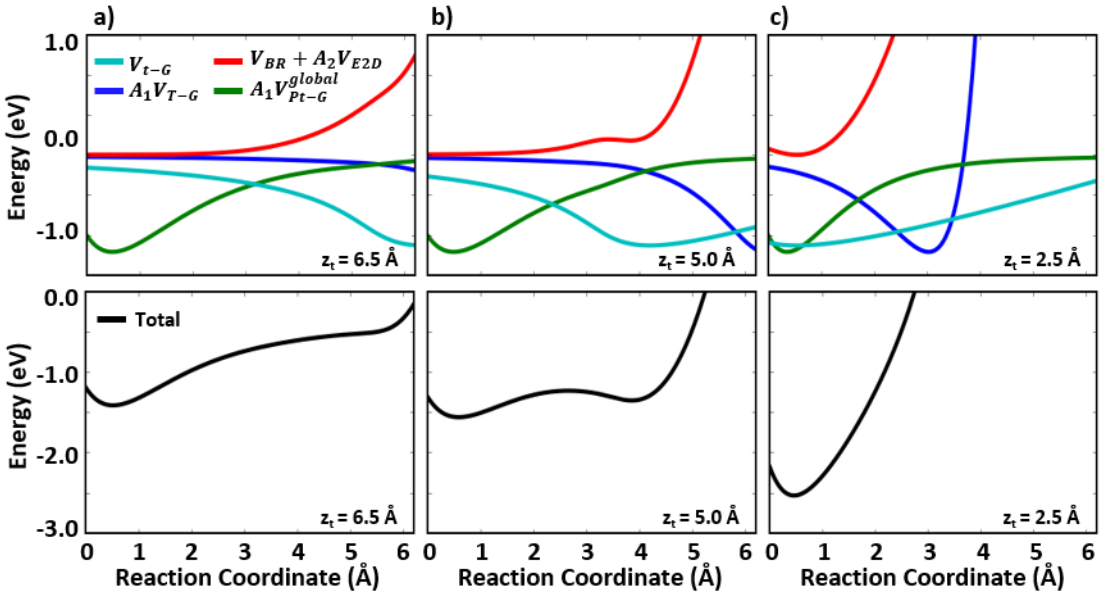

Figure S4. Decomposed (upper row) and total (bottom row) energy as a function of the reaction coordinates for tip-G distance (z_t) a) 6.5 Å, b) 5.0 Å, and c) 2.5 Å.

References

[1] I. Horcas, R. Fernandez, J. M. Gomez-Rodriguez, J. Colchero, J. Gomez-Herrero and A. M. Baro, Rev. Sci. Instrum **78**, 013705 (2007).

[2] A.J. Martínez-Galera and J.M. Gómez-Rodríguez, J. Phys. Chem. C **115**, 23036 (2011).

[3] J. P. Cleveland, S. Manne, D. Bocek and P. K. Hansma, Rev. Sci. Instrum **64**, 403 (1993).

[4] A. Labuda, Y. Miyahara, L. Cockins, and P. H. Grütter, Phys. Rev. B **84**, 125433 (2011).

[5] T. Ozaki, Phys. Rev. B **67**, 155108 (2003).

[6] S. Grimme, J. Antony, S. Ehrlich and H. Krieg, J Chem Phys **132**, 154104 (2010).

[7] C. Lee, X. D. Wei, J. W. Kysar and J. Hone, Science **321**, 385 (2008).